ACS SENSORS

pubs.acs.org/acssensors

Article

Electrochemical Impedance-Based Biosensors for the Label-Free Detection of the Nucleocapsid Protein from SARS-CoV-2

Hana Cho, Suhyun Shim, Won Woo Cho, Sungbo Cho, Hanseung Baek, Sang-Myung Lee,* and Dong-Sik Shin*

Cite This: *ACS Sens.* 2022, 7, 1676−1684

Read Online

ACCESS | Metrics & More | Article Recommendations | Supporting Information

ABSTRACT: Diagnosis of coronavirus disease (COVID-19) is important because of the emergence and global spread of severe acute respiratory syndrome coronavirus 2 (SARS-CoV-2). Real-time polymerase chain reaction (PCR) is widely used to diagnose COVID-19, but it is time-consuming and requires sending samples to test centers. Thus, the need to detect antigens for rapid on-site diagnosis rather than PCR is increasing. We quantified the nucleocapsid (N) protein in SARS-CoV-2 using an electro-immunosorbent assay (El-ISA) and a multichannel impedance analyzer with a 96-interdigitated microelectrode sensor (ToAD). The El-ISA measures impedance signals from residual detection antibodies after sandwich assays and thus offers highly specific, label-free detection of the N protein with low cross-reactivity. The ToAD sensor enables the real-time electrochemical detection of multiple samples in conventional 96-well plates. The limit of detection for the N protein was 0.1 ng/mL with a detection range up to 10 ng/mL. This system did not detect signals for the S protein. While this study focused on detecting the N protein in SARS-CoV-2, our system can also be widely applicable to detecting various biomolecules involved in antigen−antibody interactions.

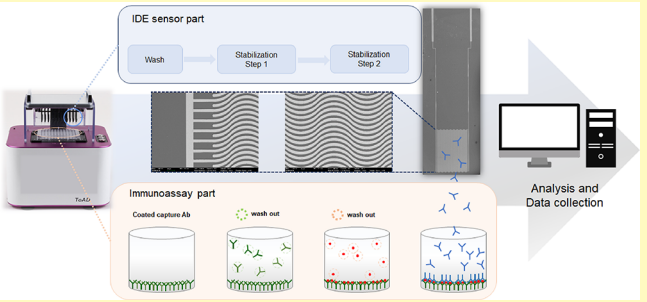

KEYWORDS: *electrochemical sensor, nucleocapsid protein, SARS-CoV-2, impedance, label-free detection*

The disease caused by severe acute respiratory syndrome coronavirus 2 (SARS-CoV-2) that emerged in 2019 and spread globally is officially named COVID-19 by The World Health Organization.[1,2] Due to the recent advent of highly contagious mutations and the increase in asymptomatic infections, a rapid antigen diagnosis is urgently needed.[3−5]

Several diagnostic and detection methods have been developed to help prevent the spread of the virus. Real-time polymerase chain reaction (RT-PCR) is a popular method for the rapid and reliable quantitation of mRNA transcription.[6] It is fast and effective and can quantify gene or transcript numbers of target sequences within a mixed community background in environmental samples with high specificity and sensitivity.[7−9] However, PCR tests are expensive because they require gene amplification equipment and diagnosis requires several hours. Paradoxically, RT-PCR is also so sensitive that trace amounts of DNA left remaining from a previous test or impurities can lead to erroneous results.[10,11]

On the other hand, immunological assays focusing on the detection of viral antigens such as the SARS-CoV-2 nucleocapsid (N) protein or spike (S) protein are currently emerging for the diagnosis of viral infection. A sandwich assay is generally used for antigen detection.[12,13] The capture and detection antibodies that are applied to measure antigens are generally referred to as antibody pairs. After an antigen binds to a capture antibody on a solid substrate, the detection antibody conjugated with appropriate reporters binds to an additional epitope on the target antigen, resulting in electrochemical or optical signal production.[14] The signal intensity indicates the amount of detection antibody, which is proportional to the antigen. Sandwich assays are highly specific and sensitive because two antibodies are required to bind to the protein. Lateral flow sandwich assays (LFAs) colorimetrically indicate an antigen that binds to an antibody and thus identify the presence or absence of a desired target.[15] Although LFAs can be purchased over the counter at pharmacies as a rapid kit with the advantage of direct application by prospective patients, these assays need to be highly specific and sensitive for general use.[16]

Electrochemical biosensors are popular analytical devices used for transducing enzymatic reactions and molecular recognition for point-of-care diagnosis.[17−22] Current commercial electrochemical biosensors are inexpensive, highly

Received: February 11, 2022
Accepted: May 19, 2022
Published: June 2, 2022

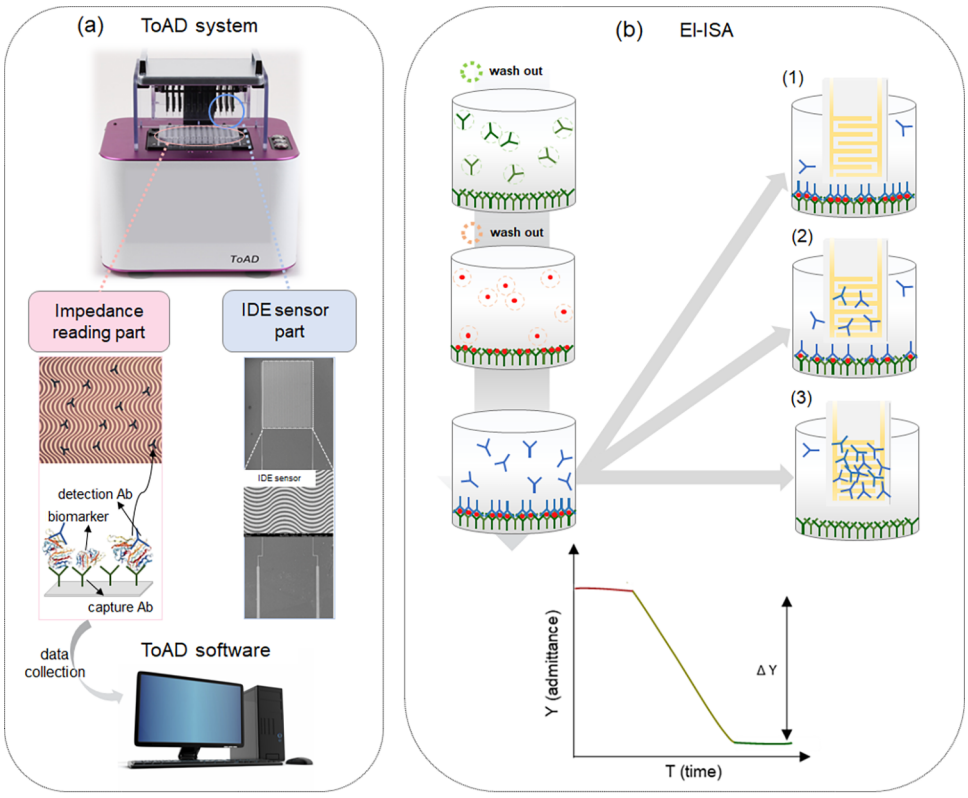

Figure 1. Operation of the ToAD system. (a) Configuration of the ToAD system consisting of an IDE sensor, impedance reader, and software to analyze real-time impedance. (b) El-ISA.

sensitive, and easy to automate. Electrochemical impedance-based biosensors might serve as attractive sensing platforms because detection is label-free.[23−26] Interdigitated microelectrodes have also attracted interest in the fields of impedimetric immunosensing and biosensing small molecules or DNA.[27] However, nonspecific protein binding on electrodes hampers the transduction of specific binding results.[28]

We propose a novel electro-immunosorbent assay (El-ISA) for detecting the N protein in SARS-CoV-2 using an impedance analyzer (ToAD) that is free of interference from nonspecific biomolecules. The target is the N protein because it is the most abundant protein in SARS-CoV-2. A capture anti-N protein Ab is immobilized to the wells of 96-well plates. The N protein binds to the capture antibody, and then the antigen is washed out. Incubation with the anti-N protein detection Ab results in sandwich formation, and the concentration of the detection antibody decreases. The El-ISA quantifies the amount of the detection antibody remaining after antigen−antibody binding without the need for labeling or catalysts such as nanoparticles or enzymes. Because the detection antibody is attached to the electrode sensing area in a fresh solution, signals are not interrupted during the collection of impedance data. In contrast, most electrochemical sensing approaches are applied to bound antigens in complex solutions such as blood and saliva containing nonspecific biomolecules, which leads to signal interruption.[29,30] The ToAD system monitors the impedance fluctuation of signals in an electric field using a 96-well platform with software displaying electrical signals including capacitance, conductance, admittance, and impedance. Combining ToAD with the El-ISA allows quantification of antigen−antibody interactions in 96-well plates by monitoring admittance in real time.

Materials and Instruments. Protein-free blocking buffer, 96-well plates, and Alexa Fluor 647 protein labeling kit were obtained from Thermo Fisher Scientific (Waltham, MA, USA). Bovine serum albumin (BSA) was purchased from GenDEPOT (Baker, Texas, USA). PBS (1×) was obtained from Corning (Corning, NY, USA). H_2O_2 (30% aqueous solution) and sodium hydroxide were purchased from Daejung Chemicals (Siheung-si, Gyeonggi-do, Korea). SARS-CoV-2 nucleocapsid protein (N protein) and anti-nucleocapsid protein antibodies (anti-N protein Ab: C524 for the capture antibody and C706 for the detection antibody) of SARS-CoV-2 were purchased from HyTest (Turku, Finland). All other reagents including casein blocking buffer (10×) were purchased from Sigma Aldrich (St. Louis, MO, USA). Fluorescence emission was measured using a SpectraMax i3x microplate reader (SpectraMax i3x, Molecular Devices, San Jose, CA, USA). The ToAD system was manufactured by Cantis Inc. (Ansan-si, Gyeonggi-do, Korea).

Stabilization of Admittance in the ToAD System. Before El-ISA evaluation with the ToAD system, electrodes in the wells of 96-well plates were immersed in 5% H_2O_2 (250 μL) for 1 h and then rinsed with deionized (DI) water (280 μL). Thereafter, 100 mM NaOH (250 μL) was added to each well and admittance was measured by the ToAD system for 2 h at a frequency of 100 Hz to monitor bleaching of the residue from the electrodes. The NaOH solution was replaced twice with PBS (250 μL), and the admittance at 100 Hz frequency was measured for 1 h.

Sandwich Assay for the El-ISA. Fluctuations in the admittance of the anti-N protein detection Ab (C706) were monitored to verify the performance of the ToAD system. After stabilization, admittance at 100 Hz was measured in real

https://doi.org/10.1021/acssensors.2c00317
ACS Sens. 2022, 7, 1676−1684

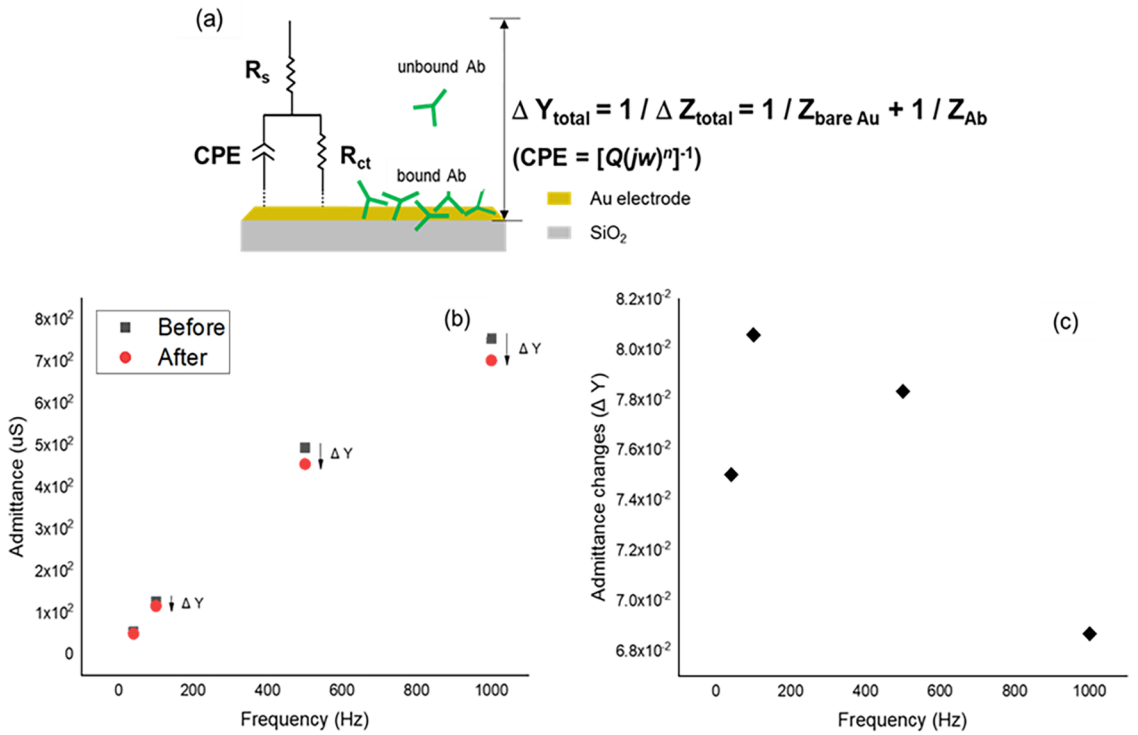

Figure 2. Determination of optimal frequency for electrochemical measurement. (a) Schematic of admittance change in the equivalent circuit dependent on the antibody adhered to the electrode. (b) Admittance magnitude before and after IgG binding on IDE electrodes at 40, 100, 500, and 1000 Hz. (c) Normalized admittance differences.

time at various concentrations of anti-N protein Ab (0, 0.1, 0.5, 1, 5, 10, and 20 ng/mL). The microwells of 96-well plates were incubated for 2 h with 2 μg/mL capture anti-N protein Ab in PBS (250 μL). The antibody was removed, and then microwells were incubated with casein (0.1×, 270 μL) blocking buffer for 1 h. The microwells were then washed with PBST (0.1% Tween 20 in PBS, 280 μL) with the plates shaking for 2 min at 500 rpm.[31,32] Subsequently, the wells were washed twice with 280 μL of PBS for 2 min with shaking at 500 rpm and then incubated with 250 μL of PBS containing 0, 0.1, 0.5, 1, 5, and 10 ng/mL N protein for 1 h. After that, the plates were again washed with PBST and PBS, and 250 μL of anti-N protein detection Ab (20 ng/mL) in PBS was added.[33] The residual detection antibody was immediately quantified using the ToAD.

Verification of Antigen−Antibody Reaction Using Fluorescence Immunoassays (FIAs). The detection antibody was labeled with Alexa 647 protein using FIA kits as described by the manufacturer. The N protein was immobilized on the anti-N protein capture Ab in 96-well plates, and the plates were washed with PBST and PBS and then incubated with 20 ng/mL labeled detection antibody in PBS for 1 h.[34,35] Fluorescence emission was measured using a SpectraMax i3x microplate reader at excitation and emission wavelengths of 647 and 668 nm, respectively. The fluorescence intensity was measured five times per well, and average values were plotted.

RESULTS AND DISCUSSION

Multichannel Impedance Analyzer with an Interdigitated Microelectrode (IDE) Sensor, ToAD. The multichannel impedance analyzer, ToAD, is a real-time, high-throughput impedance reader recently developed by Cantis Inc. (Figure 1a). It consists of a 96-IDE array corresponding to the wells of standard 96-microwell plates on the upper sensor part and an impedance reader on the lower part of the device. Electrical measurements associated with specific biological events were taken by dipping the electrode arrays into the wells. Then, electrical signals, including impedance, admittance, conductance, and phase, were wirelessly transferred in real time to ToAD software on a desktop computer (Figures S1 and S2). The ToAD system has an interdigitated wave-shaped electrode (IWE) sensor[36] that increases the uniformity of the electric field around the electrode and improves the analytical sensitivity of impedance biosensors,[37,38] which accounts for the excellent performance of the El-ISA strategy.

El-ISA. The El-ISA is based on a combination of immunological back-titration and electrochemical real-time readout by ToAD (Figure 1b). The working principle of the El-ISA can be explained as electrical quantitation (admittance changes) of the detection antibody remaining in solution after antigen−capture antibody binding. This method can be applied utilizing most commercially available ELISA kits because the operational procedure of the El-ISA is simple. It consists of a conventional immunoassay including capture antibody immobilization, blocking, antigen binding, and detection antibody incubation in 96-well plates, followed by IDE sensor dipping and real-time measurement of changes in impedance on detection antibody binding to the surfaces of gold electrodes.

Because specific immunoassays and electrical measurements are spatiotemporally separate, the El-ISA offers several advantages. Surface modification of gold sensor electrodes is not required to capture a specific target and prevent the nonspecific binding of abundant proteins in biological fluids, unlike conventional electrochemical biosensors. Here, residual

https://doi.org/10.1021/acssensors.2c00317
ACS Sens. 2022, 7, 1676−1684

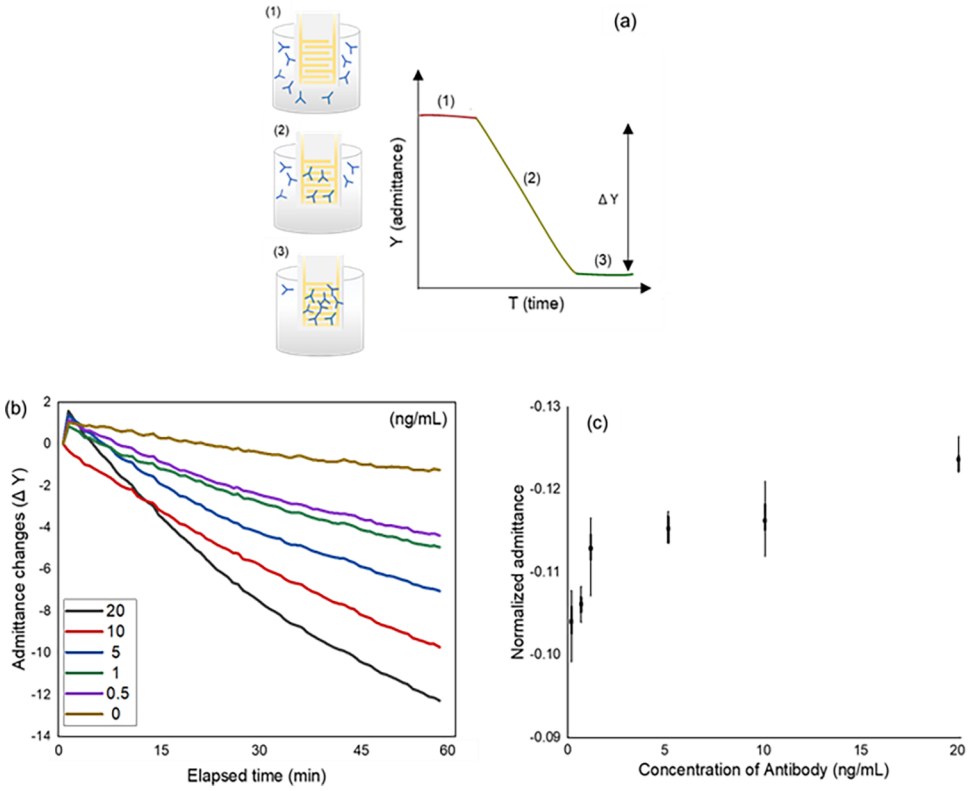

Figure 3. Measurement of anti-N protein detection Ab concentration. (a) Physisorption of the detection antibody to the electrode surface decreases admittance. (b) Admittance monitored for 60 min. Data from an array with eight electrodes were collected and averaged. (c) Normalized admittance at 60 min.

detection antibody molecules remaining after an immunoassay are directly captured on bare gold electrodes. An active bare gold surface effectively captures proteins such as antibodies,[39] and there are no other biomolecules in the solution to cause impedance changes in the IDE sensors by surface binding. This feature is an important advantage in terms of the reusability of gold IDE sensors as the electrodes can be simply cleaned, regenerated, and recycled >30 times for immunoassays. This might be an asset for commercialization (Figure S3). Moreover, the El-ISA is much simpler and more efficient than conventional ELISAs because enzymes such as horseradish peroxidase and alkaline phosphatase do not participate in signal transduction and residual detection antibody binding to the electrodes directly produces electrical signals such as admittance changes.

Determination of the Frequency for Electrochemical Measurement. The ToAD analysis software is coded based on the interfacial impedance model of an equivalent circuit composed of a constant phase element (CPE) and series solution resistance (Rs). Basically, it can measure and plot electrical parameters, including admittance, impedance, capacitance, and phase, at 40, 100, 500, and 1000 Hz in real time. The equivalent circuit shows that the detection IgG antibodies form a single layer that simply adheres to the electrode surface (Figure 2a). This interaction between IgGs and the electrode surface influences the electrical change of the interface, which is associated with double layer capacitance and charge transfer resistance. We added 20 ng/mL IgG to the electrodes to optimize the frequency. Figure 2b shows the plots of admittance magnitude before and after IgG binding to the IDE electrodes at 40, 100, 500, and 1000 Hz. The magnitude difference increased as the frequency increased from 40 to 1000 Hz, but the vertex of the corresponding normalized values was confirmed at 100 Hz (Figure 2c). The collector power (Vcc) and frequency were 0.3 mV and 100 Hz for data acquisition, respectively. The data were collected based on impedance and converted into parameters of admittance, capacitance, and conductance according to the equations designed in the software.

Stabilization of Electrical Signals from the 96-Electrode Array. The 96-electrode array was immersed in 5% H_2O_2 overnight and then washed with 100 mM NaOH on the following day for 2 h. The NaOH was replaced with PBS (working buffer) twice for 1 h each to stabilize electrical signals. Admittance obviously changed in the first stabilization step but changed minimally (138−139 μS) in the second step (Figure S4). The electrical measurements started when the change in admittance stabilized at $\leq$3 μS.

Admittance Monitoring According to Antibody Binding to Electrodes. The El-ISA records the electrical signals for the residual detection antibody to assess the antigen−antibody interaction. Therefore, we monitored anti-N protein detection Ab to verify antibody binding to the electrode before starting the El-ISA. The anti-N protein Ab gradually moves toward and physically adsorbs onto the electrode, which decreases admittance (Figure 3a); this change in admittance is referred to as ΔY. After the admittance signals stabilized, anti-N protein Ab (0−20 ng/mL) was dispensed into 96-well plates and admittance was monitored (Figure S5) for 60 min (Figure 3b). When the 96-well plate containing the residual antibody solution was loaded after the stabilization step, the admittance of the transitional state may be initially unstable after the

https://doi.org/10.1021/acssensors.2c00317
ACS Sens. 2022, 7, 1676−1684

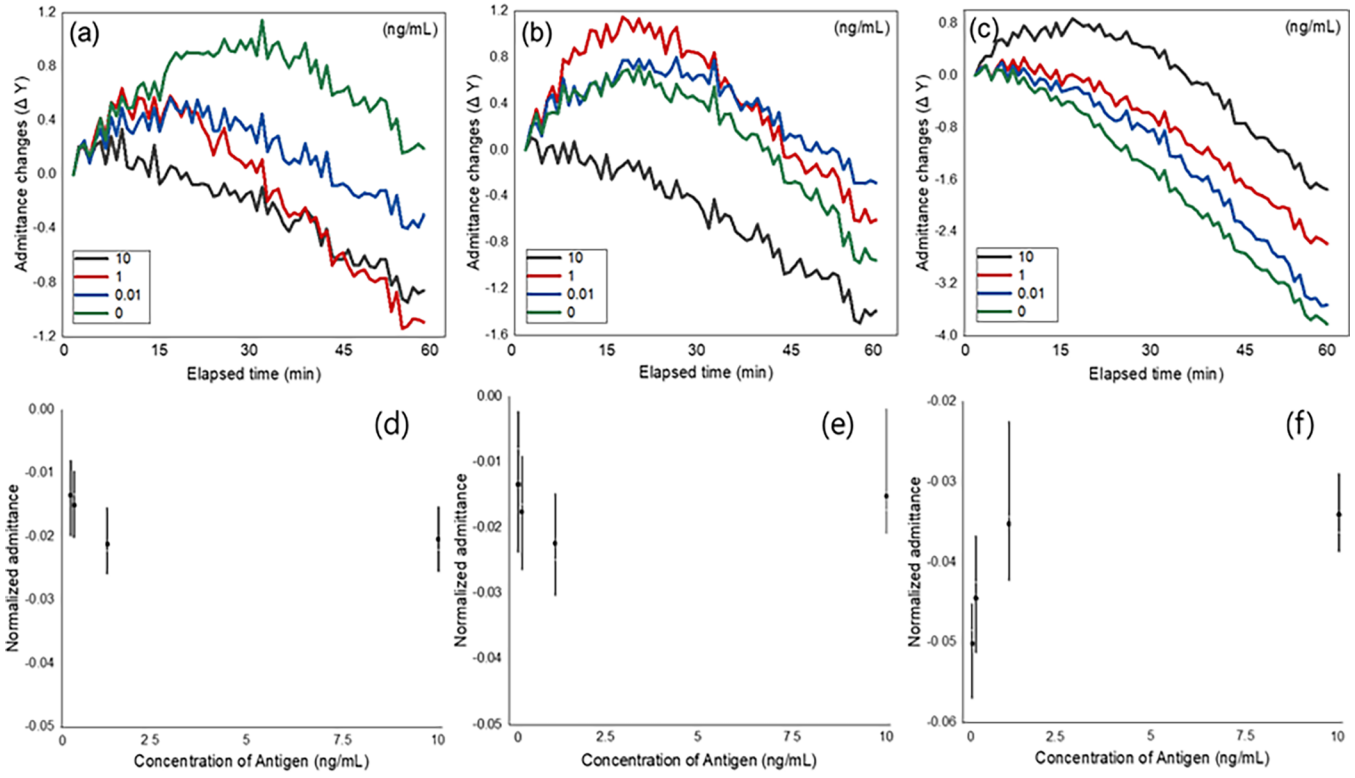

Figure 4. Optimization of blocking buffer for the El-ISA. Admittance of residual detection antibody was monitored for 1 h during the El-ISA with (a) nonprotein blocking buffer, (b) BSA (0.1×), and (c) casein (0.1×). (d–f) Normalized values of admittance in antigen–antibody reactions containing 0, 0.01, 1, and 10 ng/mL N protein, respectively.

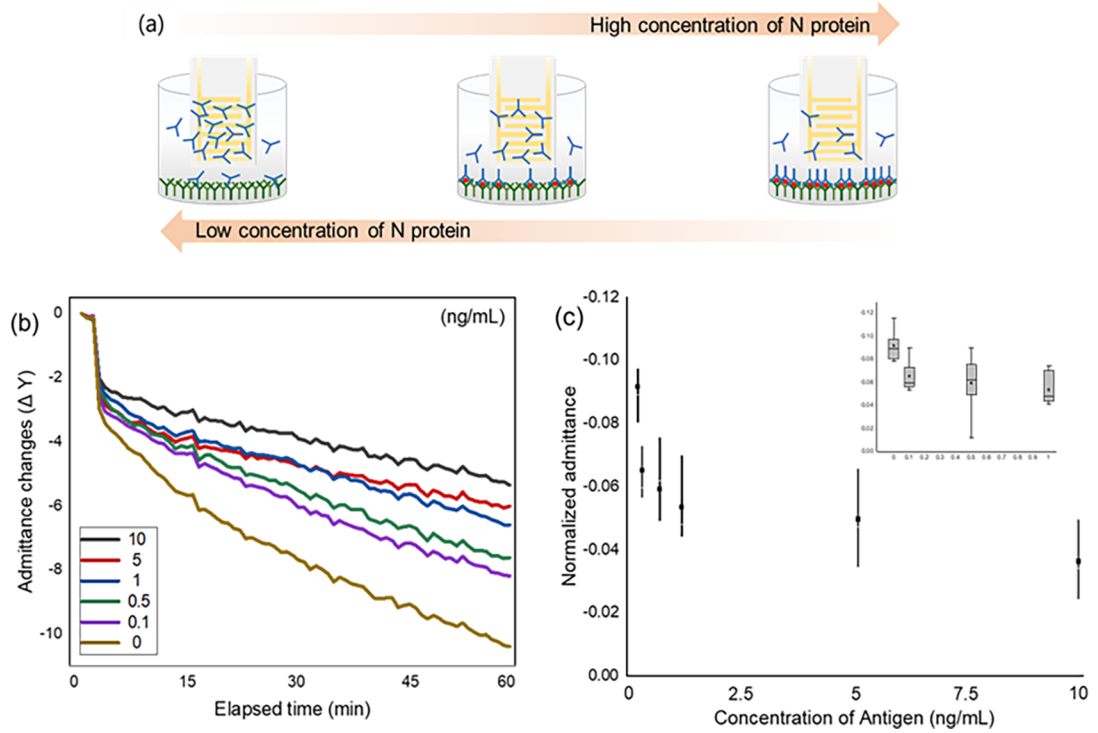

Figure 5. Principle of the El-ISA and quantification of the residual detection antibody. (a) Principle of the El-ISA depends on N protein concentration. A higher concentration of N protein results in less residual detection antibody and consequently higher electrode impedance and lower admittance. (b) Admittance of the residual detection antibody monitored in solution during the El-ISA in antigen–antibody reactions containing 0, 0.1, 0.5, 1, 5, and 10 ng/mL N protein. (c) Normalized admittance values were calculated at 1 h.

change of the solution. The first point of admittance in 10 ng/mL differed from those of other concentrations; however, it soon stabilized and showed a stable curve starting from 15 min. The admittance decreased as the antibody concentration

https://doi.org/10.1021/acssensors.2c00317
ACS Sens. 2022, 7, 1676–1684

increased because the antibody interfered with the flow of the current. Admittance was plotted at 60 min as a function of the anti-N protein Ab concentration (Figure 3c). In addition, Ab adsorption onto the electrode was evaluated using anti-N protein detection Ab labeled with Alexa Fluor 647. The fluorescence emission confirmed that the antibody was adsorbed onto the electrode, not onto the SiO_2 surface (Figure S6).

Evaluation of the El-ISA for the N Protein with the ToAD System. An optimized blocking agent was required to suppress nonspecific biomolecule binding to ensure the sensitivity and reproducibility of the El-ISA. Since the blocking agent may detach from the 96-well surface during detecting the residual antibody, we expected that a suitable blocking agent should not interfere in signal detection during immunoassays. We assessed a protein-free blocking buffer, BSA (0.1×), and casein (0.1×) solution as candidates before adding the N protein to the El-ISA. After the antigen−antibody reaction, the remaining detection antibody induced an admittance change. Casein (0.1×) inhibited nonspecific binding to the surface and stabilized the antigen−antibody interaction on the surface the most effectively compared to the other candidates, which resulted in the most stable change in admittance (Figure S7 and Figure 4). The protein-free blocking buffer and BSA did not sufficiently block nonspecific binding for the El-ISA. Anti-N protein Ab remaining after the antigen−antibody reaction was quantified by blocking with casein in subsequent studies.

Changes in admittance were monitored with 0−10 ng/mL N-protein. A higher N protein concentration induces more antibody−antigen−antibody reaction on the 96-well plate. Thus, the sandwich formation is strongly induced, resulting in less detection antibody remaining in the solution. Since there are few detection antibodies to physically adsorb to the electrode, the impedance and the admittance do not change significantly. In contrast, in the case of lower N protein concentration, the less sandwich formation induces more detection antibody remaining in the solution. Thus, the impedance and the admittance change prominently (Figure 5a). Considering these criteria, we determined changes in real-time admittance values with physisorption of the residual detection antibody in the solution (Figure 5b). Admittance was plotted as a function of the N protein concentration at 60 min (Figure 5c). The results confirmed that the El-ISA can quantify N protein concentrations by monitoring admittance. Table 1 lists a summary of SARS-CoV-2 detection methods, and the performance of our ToAD system is comparable with those of other electrochemical detecting systems.

Specificity of the El-ISA with ToAD for the N Protein. We validated the cross-reactivity of anti-N protein Ab against 1 ng/mL S protein in the El-ISA. The admittance of the El-ISA did not significantly change with these concentrations of S protein, but it obviously changed according to the N protein concentration (Figure 6a,b). In particular, we established a specificity test using sample solutions mixed with the N and S proteins. The N protein (1 ng/mL) was consistently quantified regardless of the concentrations of the S protein (0, 1, 10, and 20 ng/mL) (Figure 6c). These results indicated that the El-ISA was specific for the N protein of SARS-CoV-2 compared with the S protein.

We used the ToAD system to analyze 20% human serum spiked with N protein to determine the feasibility of the El-ISA for clinical applications. Figure 7 shows residual anti-N protein Ab concentrations at 60 min. The spiked serum did not

Table 1. Summary of the Electrochemical SARS-CoV-2 Detection Methods

	methods of SARS-CoV-2 detection						
	voltammetry[19,20]		potentiometry[21,23]		electrical impedance spectroscopy[22]		this work
target	S protein, N protein	spike antigen	spike S1 protein	spike protein	S1 (S protein)		N protein
detection limit	19 ng/mL and 8 ng/mL	1 pg/mL	1 fg/mL	1.6×10^{1} pfu/mL	2.8×10^{-15} M		0.1 ng/mL
linear range	0.04−10 μg/mL	1 pg/mL to 10 ng/mL	10 fg/mL to 1 μg/mL	1 fg/mL to 10 pg/mL	0.01 fM to 30 nM		0.1−10 ng/mL
selectivity	no cross-reactivity with influenza A (H1N1) and influenza 2009 pH1N1	no cross-reactivity with MERS-CoV, influenza A, and Pneumoniae	no cross-reactivity with the N protein	no cross-reactivity with MERS-CoV	no cross-reactivity with the RBD antibody, N antibody, and IL-6 protein		no cross-reactivity with the S protein

https://doi.org/10.1021/acssensors.2c00317
ACS Sens. 2022, 7, 1676−1684

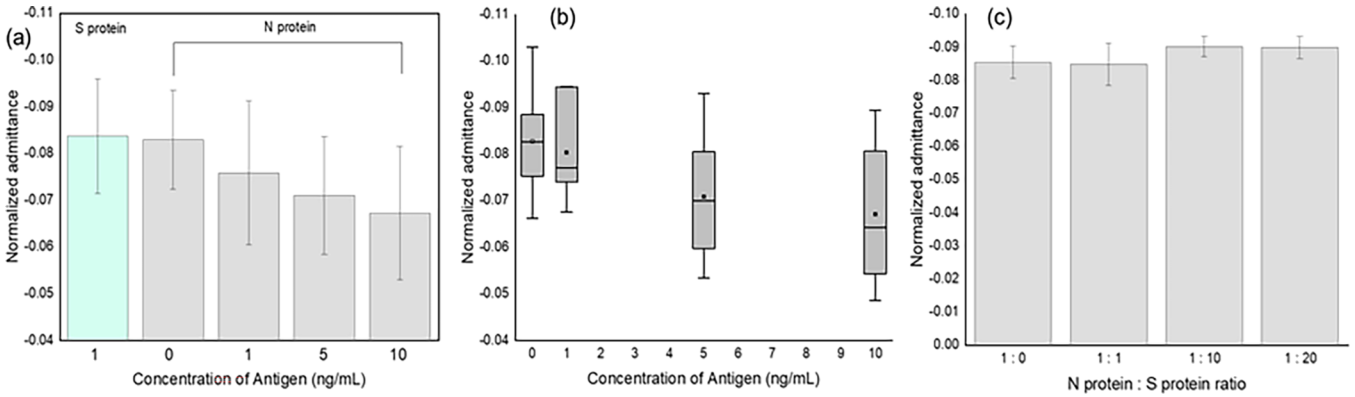

Figure 6. Specificity of the El-ISA for the N protein compared with that for the S protein. (a) Changes in admittance of S (1 ng/mL) and N (0, 1, 5, and 10 ng/mL) proteins normalized at 60 min (b) Normalized admittance values for the N protein at 1 h. (c) Normalized admittance using a mixed solution of N and S proteins.

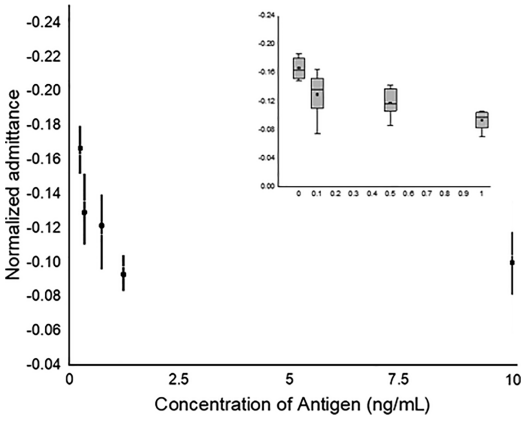

Figure 7. Specificity of the El-ISA determined in 20% human serum spiked with N protein. Concentrations of spiked N protein: 0, 0.1, 0.5, 1, and 10 ng/mL.

interfere with the El-ISA, indicating excellent potential for analyzing clinical samples. These results supported our primary claim regarding the El-ISA because eliminating impurities allowed measurements of detection antibody admittance without interference.

FIA of the N Protein of SARS-CoV-2. We investigated the reliability of the N protein results of the ToAD system using FIAs to detect antibody on the bottoms of microwells (Figure 8a). After the sandwich assay, the fluorescently labeled detection antibody was quantified using the SpectraMax i3x microplate reader. The fluorescence intensity emitted by the S protein was not significant; however, that emitted by the N protein was linear and concentration-dependent (Figure 8b,c). This association was also linear in 20% human serum spiked with N protein (Figure 8d). These results confirmed that our immunoassay system can be applied to clinical analyses.

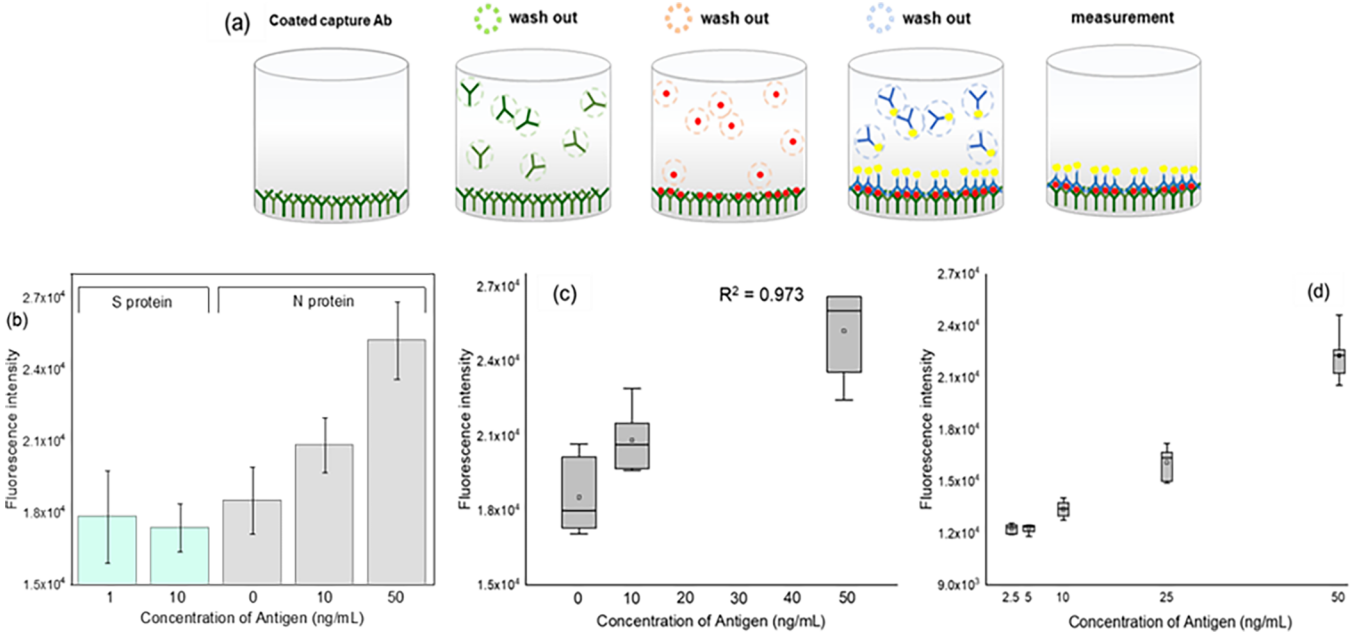

Figure 8. FIA of the N protein to cross-validate ToAD specificity. (a) Procedure for N protein detection by the FIA. (b) N and S proteins determined by the FIA. (c) Fluorescence intensity according to N protein concentrations. (d) FIA in 20% human serum spiked with various N protein concentrations.

https://doi.org/10.1021/acssensors.2c00317
ACS Sens. 2022, 7, 1676−1684

CONCLUSIONS

We designed a real-time system to monitor and detect the N protein of SARS-CoV-2 by combining the El-ISA with ToAD. We optimized the measurement frequency, electrode regeneration, and the blocking method before detecting the N protein using our label-free El-ISA with an LOD of 0.1 ng/mL, a range extending to 10 ng/mL, and minimal cross-reactivity with S protein. The assay also detected the N protein in spiked 20% human serum. Our FIA data also confirmed that our system was sensitive and specific for detecting the N protein. Moreover, the ToAD system can detect individual electrochemical signals in 96-well plates in real time. This novel El-ISA combined with ToAD is an economical, rapid, convenient system that is simple to operate. We therefore envision that this combination could serve not only as a cost-effective, large-scale test for detection of SARS-CoV-2 but also as a general platform for the real-time measurement of other biomolecules in clinical samples.

ASSOCIATED CONTENT

Supporting Information

The Supporting Information is available free of charge at https://pubs.acs.org/doi/10.1021/acssensors.2c00317.

ToAD system and 96-electrode arrays; structure of IWEs; results of reusing the system (electrodes); stabilization step in the system; monitoring of detection anti-N protein Ab with software; labeled antibody onto a pattern of the Au electrode; comparison of blocking buffers in the El-ISA by software dependent on N protein concentration (PDF)

AUTHOR INFORMATION

Corresponding Authors

Sang-Myung Lee − *Cantis Inc., Ansan-si, Gyeonggi-do 15588, Republic of Korea*; Email: smlee@cantis.co.kr

Dong-Sik Shin − *Department of Chemical and Biological Engineering and Industry Collaboration Center, Sookmyung Women's University, Seoul 04310, Republic of Korea*; orcid.org/0000-0001-8101-0793; Email: dshin@sm.ac.kr

Authors

Hana Cho − *Department of Chemical and Biological Engineering and Industry Collaboration Center, Sookmyung Women's University, Seoul 04310, Republic of Korea*

Suhyun Shim − *Department of Chemical and Biological Engineering, Sookmyung Women's University, Seoul 04310, Republic of Korea*

Won Woo Cho − *Cantis Inc., Ansan-si, Gyeonggi-do 15588, Republic of Korea*

Sungbo Cho − *Department of Electronics Engineering, Gachon University, Seongnam-si, Gyeonggi-do 13120, Republic of Korea*; orcid.org/0000-0003-3839-6410

Hanseung Baek − *Comprehensive Dental Care Center, Purme Nexon Children Rehabilitation Hospital, Seoul 03918, Republic of Korea*

Complete contact information is available at: https://pubs.acs.org/10.1021/acssensors.2c00317

Author Contributions

H.C. contributed to conceptualization, methodology, formal analysis, investigation, data curation, and writing (original draft). S.S. contributed to methodology, formal analysis, investigation, and data curation. W.W.C. contributed to conceptualization, resources, supervision, funding acquisition, and writing (review and editing). S.C. contributed to formal analysis, supervision, and writing (review and editing). H.B. contributed to supervision and writing (review and editing). S.-M.L. contributed to conceptualization, resources, supervision, funding acquisition, writing (review and editing), and project administration. D.-S.S. contributed to conceptualization, resources, supervision, funding acquisition, writing (review and editing), and project administration.

Notes

The authors declare no competing financial interest.

ACKNOWLEDGMENTS

This research was supported by the research fund of the National Research Foundation of Korea (NRF) grant funded by the Korea government (Ministry of Science and ICT) (NRF-2019R1F1A1062208), the Ministry of Trade, Industry and Energy (Grant No. 20015793), Commercialization Promotion Agency for R&D Outcomes (Grant No. 2021-0036), the Korea Health Industry Development Institute (KHIDI, grant number: HU21C0098), and Purme Nexon Children Rehabilitation Hospital.

REFERENCES

(1) Shereen, M. A.; Khan, S.; Kazmi, A.; Bashir, N.; Siddique, R. COVID-19 infection: Origin, transmission, and characteristics of human coronaviruses. *J. Adv. Res.* **2020**, *24*, 91−98.

(2) Munnoli, P. M.; Nabapure, S.; Yeshavanth, G. Post-COVID-19 precautions based on lessons learned from past pandemics: a review. *J. Public Health* **2022**, 1−9.

(3) Chakraborty, I.; Maity, P. COVID-19 outbreak: Migration, effects on society, global environment and prevention. *Sci. Total Environ.* **2020**, *728*, No. 138882.

(4) Xu, L.; Li, D.; Ramadan, S.; Li, Y.; Klein, N. Facile biosensors for rapid detection of COVID-19. *Biosens. Bioelectron.* **2020**, *170*, No. 112673.

(5) Yuki, K.; Fujiogi, M.; Koutsogiannaki, S. COVID-19 pathophysiology: A review. *Clin. Immunol.* **2020**, *215*, No. 108427.

(6) Rai, P.; Kumar, B. K.; Deekshit, V. K.; Karunasagar, I.; Karunasagar, I. Detection technologies and recent developments in the diagnosis of COVID-19 infection. *Appl. Microbiol. Biotechnol.* **2021**, *105*, 441−455.

(7) Smith, C. J.; Osborn, A. M. Advantages and limitations of quantitative PCR (Q-PCR)-based approaches in microbial ecology. *FEMS Microbiol. Ecol.* **2009**, *67*, 6−20.

(8) Kaltenboeck, B.; Wang, C. Advances in real-time PCR: application to clinical laboratory diagnostics. *Adv. Clin. Chem.* **2005**, *40*, 219−259.

(9) Radonić, A.; Thulke, S.; Mackay, I. M.; Landt, O.; Siegert, W.; Nitsche, A. Guideline to reference gene selection for quantitative real-time PCR. *Biochem. Biophys. Res. Commun.* **2004**, *313*, 856−862.

(10) Loeffelholz, M. J.; Tang, Y.-W. Laboratory diagnosis of emerging human coronavirus infections - the state of the art. *Emerg. Microbes Infect.* **2020**, *9*, 747−756.

(11) Vashist, S. K. In Vitro Diagnostic Assays for COVID-19: Recent Advances and Emerging Trends. *Diagnostics* **2020**, *10*, 1−7.

(12) Li, T.; Wang, L.; Wang, H.; Li, X.; Zhang, S.; Xu, Y.; Wei, W. Serum SARS-COV-2 Nucleocapsid Protein: A Sensitivity and Specificity Early Diagnostic Marker for SARS-COV-2 Infection. *Front. Cell Infect. Microbiol.* **2020**, *10*, 470.

(13) Smithgall, M. C.; Dowlatshahi, M.; Spitalnik, S. L.; Hod, E. A.; Rai, A. J. Types of Assays for SARS-CoV-2 Testing: A Review. *Lab. Med.* **2020**, *51*, 59−65.

(14) Yuan, M.; Liu, H.; Wu, N. C.; Lee, C. D.; Zhu, X.; Zhao, F.; Huang, D.; Yu, W.; Hua, Y.; Tien, H.; Rogers, T. F.; Landais, E.; Sok, D.; Jardine, J. G.; Burton, D. R.; Wilson, I. A. Structural basis of a shared antibody response to SARS-CoV-2. *Science* **2020**, *369*, 1119−1123.
(15) Gangula, A.; Ghoshdastidar, S.; Kainth, J.; Elangovan, A.; Premkumar, K.; John, A. P.; Erica, E. B.; Upendran, A.; Kannan, R.; Hainsworth, D. P. Lateral Flow Immuno Assay for Point-of-care Screening of Retinopathy of Prematurity. *Invest. Ophthalmol. Vis. Sci.* **2019**, *60*, 6524.
(16) Posthuma-Trumpie, G. A.; Korf, J.; van Amerongen, A. Lateral flow (immuno) assay: its strengths, weaknesses, opportunities and threats. A literature survey. *Anal. Bioanal. Chem.* **2009**, *393*, 569−582.
(17) Zhou, Q.; Rahimian, A.; Son, K.; Shin, D. S.; Patel, T.; Revzin, A. Development of an aptasensor for electrochemical detection of exosomes. *Methods* **2016**, *97*, 88−93.
(18) Shin, D.-S.; Liu, Y.; Gao, Y.; Kwa, T.; Matharu, Z.; Revzin, A. Micropatterned Surfaces Functionalized with Electroactive Peptides for Detecting Protease Release from Cells. *Anal. Chem.* **2013**, *85*, 220−227.
(19) Fabiani, L.; Saroglia, M.; Galatà, G.; De Santis, R.; Fillo, S.; Luca, V.; Faggioni, G.; D'Amore, N.; Regalbuto, E.; Salvatori, P.; et al. Magnetic beads combined with carbon black-based screen-printed electrodes for COVID-19: A reliable and miniaturized electrochemical immunosensor for SARS-CoV-2 detection in saliva. *Biosens. Bioelectron.* **2021**, *171*, 1−9.
(20) Raziq, A.; Kidakova, A.; Boroznjak, R.; Reut, J.; Opik, A.; Syritski, V. Development of a portable MIP-based electrochemical sensor for detection of SARS-CoV-2 antigen. *Biosens. Bioelectron.* **2021**, *178*, 1−7.
(21) Mavrikou, S.; Moschopoulou, G.; Tsekouras, V.; Kintzios, S. Development of a Portable, Ultra-Rapid and Ultra-Sensitive Cell-Based Biosensor for the Direct Detection of the SARS-CoV-2 S1 Spike Protein Antigen. *Sensors* **2020**, *20*, 1−12.
(22) Ali, M. A.; Hu, C.; Jahan, S.; Yuan, B.; Saleh, M. S.; Ju, E.; Gao, S. J.; Panat, R. Sensing of COVID-19 Antibodies in Seconds via Aerosol Jet Nanoprinted Reduced-Graphene-Oxide-Coated 3D Electrodes. *Adv. Mater.* **2021**, *33*, 2006647.
(23) Seo, G.; Lee, G.; Kim, M. J.; Baek, S. H.; Choi, M.; Ku, K. B.; Lee, C. S.; Jun, S.; Park, D.; Kim, H. G.; et al. Rapid Detection of COVID-19 Causative Virus (SARS-CoV-2) in Human Nasopharyngeal Swab Specimens Using Field-Effect Transistor-Based Biosensor. *ACS Nano* **2020**, *14*, 5135−5142.
(24) Rashed, M. Z.; Kopechek, J. A.; Priddy, M. C.; Hamorsky, K. T.; Palmer, K. E.; Mittal, N.; Valdez, J.; Flynn, J.; Williams, S. J. Rapid detection of SARS-CoV-2 antibodies using electrochemical impedance-based detector. *Biosens. Bioelectron.* **2021**, *171*, No. 112709.
(25) Cesewski, E.; Johnson, B. N. Electrochemical biosensors for pathogen detection. *Biosens. Bioelectron.* **2020**, *159*, No. 112214.
(26) Suni, I. I. Impedance methods for electrochemical sensors using nanomaterials. *TrAC,Trends Anal. Chem.* **2008**, *27*, 604−611.
(27) Yang, L.; Li, Y.; Griffis, C. L.; Johnson, M. G. Interdigitated microelectrode (IME) impedance sensor for the detection of viable Salmonella typhimurium. *Biosens. Bioelectron.* **2004**, *19*, 1139−1147.
(28) Varshney, M.; Li, Y. Interdigitated array microelectrode based impedance biosensor coupled with magnetic nanoparticle-antibody conjugates for detection of Escherichia coli O157:H7 in food samples. *Biosens. Bioelectron.* **2007**, *22*, 2408−2414.
(29) Quoc, T. V.; Ngoc, V. N.; Bui, T. T.; Jen, C. P.; Duc, T. C. High-Frequency Interdigitated Array Electrode-Based Capacitive Biosensor for Protein Detection. *BioChip J.* **2019**, *13*, 403−415.
(30) El-Said, W. A.; Al-Bogami, A. S.; Alshitari, W.; El-Hady, D. A.; Saleh, T. S.; El-Mokhtar, M. A.; Choi, J.-W. Electrochemical Microbiosensor for Detecting COVID-19 in a Patient Sample Based on Gold Microcuboids Pattern. *BioChip J.* **2021**, *15*, 287−295.
(31) Pierangeli, S. S.; Harris, E. N. A protocol for determination of anticardiolipin antibodies by ELISA. *Nat. Protoc.* **2008**, *3*, 840−848.
(32) Zhu, M.; Gong, X.; Hu, Y.; Ou, W.; Wan, Y. Streptavidin-biotin-based directional double Nanobody sandwich ELISA for clinical rapid and sensitive detection of influenza H5N1. *J. Transl. Med.* **2014**, *12*, 352.
(33) Choi, S.; Choi, E. Y.; Kim, D. J.; Kim, J. H.; Kim, T. S.; Oh, S. W. A rapid, simple measurement of human albumin in whole blood using a fluorescence immunoassay (I). *Clin. Chim. Acta* **2004**, *339*, 147−156.
(34) Berlier, J. E.; Rothe, A.; Buller, G.; Bradford, J.; Gray, D. R.; Filanoski, B. J.; Telford, W. G.; Yue, S.; Liu, J.; Cheung, C. Y.; et al. Quantitative comparison of long-wavelength Alexa Fluor dyes to Cy dyes: fluorescence of the dyes and their bioconjugates. *J. Histochem. Cytochem.* **2003**, *51*, 1699−1712.
(35) Kuo, Y. C.; Lee, C. K.; Lin, C. T. Improving sensitivity of a miniaturized label-free electrochemical biosensor using zigzag electrodes. *Biosens. Bioelectron.* **2018**, *103*, 130−137.
(36) Ohno, R.; Ohnuki, H.; Wang, H.; Yokoyama, T.; Endo, H.; Tsuya, D.; Izumi, M. Electrochemical impedance spectroscopy biosensor with interdigitated electrode for detection of human immunoglobulin A. *Biosens. Bioelectron.* **2013**, *40*, 422−426.
(37) Chinnadayyala, S. R.; Park, J.; Abbasi, M. A.; Cho, S. Label-free electrochemical impedimetric immunosensor for sensitive detection of IgM rheumatoid factor in human serum. *Biosens. Bioelectron.* **2019**, *143*, 11642.
(38) Le, H. T. N.; Cho, S. Sensitive Electrochemical Detection of Phosphorylated-Tau Threonine 231 in Human Serum Using Interdigitated Wave-Shaped Electrode. *Biomedicines* **2022**, *10*, 1−11.
(39) Cohavi, O.; Reichmann, D.; Abramovich, R.; Tesler, A. B.; Bellapadrona, G.; Kokh, D. B.; Wade, R. C.; Vaskevich, A.; Rubinstein, I.; Schreiber, G. A quantitative, real-time assessment of binding of peptides and proteins to gold surfaces. *Chemistry* **2011**, *17*, 1327−1336.

https://doi.org/10.1021/acssensors.2c00317
ACS Sens. 2022, 7, 1676−1684